

Magnetic properties of iron-doped channels in $\text{H-Nb}_2\text{O}_5$

This article has been downloaded from IOPscience. Please scroll down to see the full text article.

2000 J. Phys.: Condens. Matter 12 2825

(<http://iopscience.iop.org/0953-8984/12/12/321>)

View [the table of contents for this issue](#), or go to the [journal homepage](#) for more

Download details:

IP Address: 171.66.16.221

The article was downloaded on 16/05/2010 at 04:42

Please note that [terms and conditions apply](#).

Magnetic properties of iron-doped channels in H-Nb₂O₅

Oswaldo F Schilling[†] and Luis Ghivelder[‡]

[†] Departamento de Física, Universidade Federal de Santa Catarina, Campus Universitário, 88040-900 Florianópolis, SC, Brazil

[‡] Instituto de Física, Universidade Federal do Rio de Janeiro, CP 68528, 21945-970, Rio de Janeiro RJ, Brazil

E-mail: osvaldof@mbx1.ufsc.br and luisghiv@if.ufrj.br

Received 7 December 1999

Abstract. H-Nb₂O₅ (Nb₂₈O₇₀) is a semiconductor whose structure is built of NbO₆ octahedra, which share corners and edges to form blocks parallel to the basal *ac* plane of the structure. One unit cell contains two blocks of 3 × 4 and 3 × 5 octahedra displaced by 1/2 *b*-axis spacing, besides one further Nb atom located in tetrahedrally coordinated sites along channels parallel to the *b* axis. Such channels contain octahedral interstices which are the preferential sites for point defect segregation in this structure. The possibility of using the channels as a framework for obtaining oriented spin arrays has never been explored in the literature. To investigate which kind of magnetic interaction would arise we manufactured a sample of H-Nb₂O₅ containing enough Fe to fill part of the octahedral interstices in the channels and measured the ac susceptibility response. The results were consistent with the formation of linear chains of spins, with variable coupling constants along the chains. The variable coupling can be understood as a consequence of the influence of the large number of possible arrangements of Nb and Fe atoms along the channels upon the sign and magnitude of superexchange interactions mediated by the oxygen atoms.

1. Introduction

The investigation of quasi-one-dimensional magnetic systems has been pursued by many groups in recent years. Most of the work in this area has concentrated on organic chain-like structures containing transition metal ions [1]. Inorganic chainlike materials, like CuGeO₃, have also been investigated in search of spin–Peierls transitions [2]. Other materials do not display such chainlike structure, but contain transition metal ions aligned along some crystallographic direction, which make them magnetically one dimensional such as VOMoO₄ [3]. The thermodynamic properties of these materials can usually be described by a Heisenberg Hamiltonian, with uniform coupling constants along the chains. However, other systems display signs of disorder in the magnetic coupling, and the analysis becomes more complex [4].

Among the compounds whose structure might potentially display one-dimensional magnetism, we chose H-Nb₂O₅ (Nb₂₈O₇₀)—hereinafter called the ‘H phase’—for the present investigation. The H phase is one of the allotropic forms of niobium pentoxide [5]. The structure is monoclinic, with unit cell dimensions $a = 2.12$ nm, $b = 0.382$ nm, $c = 1.93$ nm and $\beta = 120^\circ$. The structure is formed by blocks of corner-sharing NbO₆ octahedra in the *a*–*c* cross section [5]. The blocks are interconnected by edge-sharing octahedra, yielding two sets of columns: one with its base at $y = 0$ and the other at $y = b/2$. Each octahedron contains one Nb ion in its centre. One unit cell contains two blocks of 3 × 5 and 3 × 4 octahedra displaced along the *b* axis. Figure 1 shows the projection of this structure along

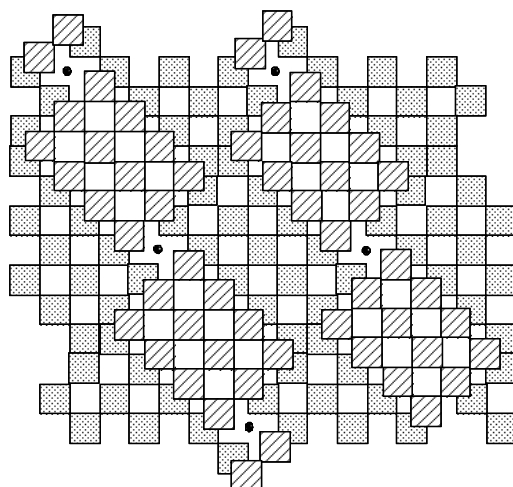


Figure 1. Projection of the H-Nb₂O₅ structure along the *b* axis. Squares represent the projections of NbO₆ octahedra linked by the corners. Note the upper blocks containing $3 \times 4 = 12$ (hatched) octahedra, and the lower blocks containing $3 \times 5 = 15$ (dotted) octahedra. The black dots represent Nb atoms in tetrahedral sites along channels parallel to the *b* axis.

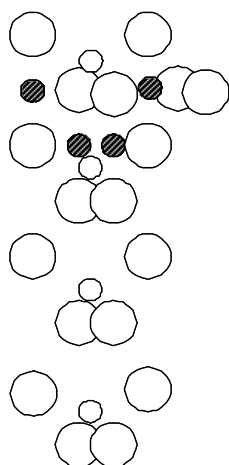


Figure 2. Side view of one of the channels of the structure. Small open circles = Nb atoms in tetrahedral sites; large open circles = oxygen atoms; dark circles = some of the free octahedral positions.

the *b* axis. As shown in the figure, the structure also contains channels between the blocks. One Nb ion per unit cell occupies a tetrahedral site at $y = b/4$ along these channels. As shown in figure 2, the channels are surrounded by octahedral interstices, which are available for filling by displaced Nb atoms or by alien ions. Anderson and co-workers [6] investigated the H phase and related compounds by electron microscopy. They showed that deviations from ideal stoichiometry in these materials could be explained simply by analysing the way octahedral sites were filled in the vicinity of the channels. The number of defects in the bulk of the octahedra blocks was found to be negligible. Motivated by such results, one of the authors calculated the thermodynamic properties of the H-phase based on the hypothesis

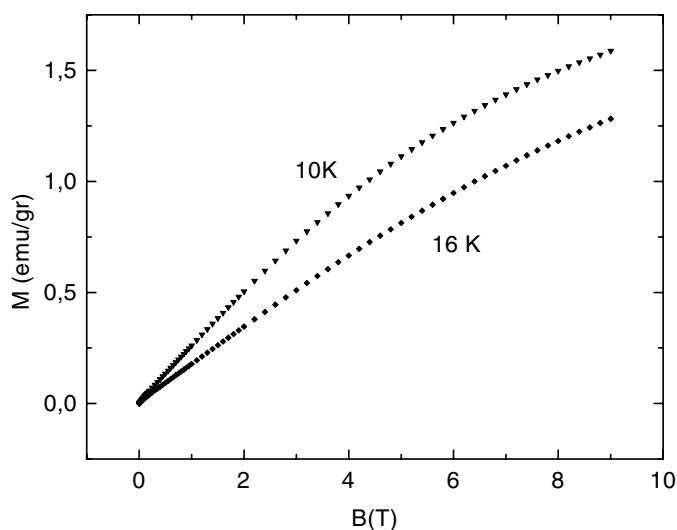


Figure 3. Magnetization–field measurements for $T = 10$ K and 16 K (to convert M to the SI units A/m multiply by 4580).

that defects existed only around the channels [7]. It was shown that, indeed, even the phase transition between the H-phase and the $\text{Nb}_{53}\text{O}_{132}$ phase might precisely be predicted simply by considering the number and distribution of vacancies in the oxygen sublattice around the channels.

Such previous information indicated that alien transition metal ions similar in size to the Nb ions might preferentially align along the channels of the H-phase structure, occupying the octahedral sites available. Another interesting perspective comes from the fact that around each tetrahedral site in a channel there are four octahedral sites. This implies that there is a number of possible arrangements of magnetic moments along the channels, with correspondingly different coupling constants. Superexchange interactions mediated by oxygen are strongly dependent on bond angles and inter-ionic distances. Therefore disordered one-dimensional magnetic arrays might be expected to form depending on doping concentration. The ac magnetic susceptibility data reported in this work are consistent with such picture.

We prepared an $H\text{-Nb}_2\text{O}_5$ sample containing enough iron to fill one octahedral site per three unit cells. The experiments involved dc magnetization and ac susceptibility measurements down to 1.8 K. Such experiments and sample preparation details are described in the next section. The interpretation of the main features of the experimental ac susceptibility data, i.e. undulations and peaks observed below 15 K, required a model for the kinetics of Fe spin flips that would account for correlations between spins. We obtained a satisfactory description of the data by analysing the magnetic response of a ring of five spins. The susceptibility for this model was obtained by solving the Glauber master equation [8] adapted by Reger and Binder [4] for inhomogeneous coupling along the ring. Albeit simple, the model reproduces all the main features observed.

2. Experimental methods

The samples were prepared by mixing chemical grade Fe_2O_3 and NbO_2 in the approximate mass proportion 1/100. Such concentration provides about one interstitial Fe ion per three

unit cells of the matrix. Admitting that the Fe ions are distributed in the channels the mean distance between two Fe ions is about 1.1 nm. The powders were thoroughly mixed and heated in a box furnace for 24 hours at 1050 °C. The H-phase is the stable form of niobium oxide at high temperature. After cooling, the powder was analysed by x-ray diffraction. The spectra displayed peaks belonging to H-Nb₂O₅ only, confirming that the structural effect of the small amount of iron added was negligible. Measurements of dc magnetization and ac susceptibility were carried out in a commercial magnetometer (Quantum Design PPMS). The ac measurements were taken with an exciting field of 10 Oe and frequencies between 1 and 10 kHz. The measurements covered temperatures down to 1.8 K and dc magnetic fields up to 9 T.

3. Experimental results

We carried out dc magnetization measurements at constant temperature to determine the Landé factor and the spin of the magnetic ions present in the sample. Figure 3 displays results for 10 and 16 K. These measurements were carried out both for increasing and decreasing field and no hysteresis was observed. The low field linear part of these plots can be fitted to Curie's law. The fits are consistent with $g = 2$ and total spin $\sigma = 2$, which implies that the iron valence is Fe²⁺ and LS coupling is overcome by crystal-field effects. The stoichiometric H-phase is a semiconductor, and displays a small temperature-independent paramagnetic susceptibility between 77 and 400 K [9]. In particular, our magnetization measurements display no sign of the presence of Nb⁴⁺ ions, usually found in non-stoichiometric, oxygen deficient, Nb compounds [9]. Therefore, we conclude that the matrix structure is acting simply as a frame where the Fe ions can be arranged along quasi-one-dimensional arrays, and neglect the presence of other magnetic ions. Our main results are the ac susceptibilities at low temperatures as a function of dc field and exciting ac field frequency. Figure 4 shows the real part χ' of the ac susceptibility for dc fields between 0.5 and 9 T, and frequency (f) of 1 kHz. Also shown are fits to a Ising ring model of five spins, to be discussed in the next section. Figure 5 shows the variation of the susceptibility with frequency for dc magnetic fields $B = 2$ and 4 T. Figure 6 shows simulated curves for several frequencies and two values of α , the spin flip attempt frequency. The low sensitivity of the data to the applied frequency is consistent with $\omega = 2\pi f \ll \alpha$. This is the case for the simulations in figure 4, in which we adopted a typical attempt frequency $\alpha \approx k_B T / h \approx 10^{10}$ Hz (h is Planck's constant).

4. Theoretical model

The main features of the susceptibility data are the undulations observed below 15 K, shown in figures 4 and 5. These undulations are the result of long-range correlations among spins in the array. In order to reproduce such behaviour we needed a model for the array and the coupling between spins. The need to restrict computational effort led us to analyse the simplest model that might be solved exactly and yet reproduce the main features of the data. Therefore, we decided to study the kinetics of spin flips in a Ising ring of $N = 5$ spins with variable coupling between nearest neighbours. Between each pair of neighbouring spins of indices $i - 1$ and i we assume a coupling constant J_{i-1} . The spin flips are induced by thermal activation and by a time-varying magnetic field $B(t) = B_0 + \delta b \exp(i\omega t)$, where $\delta b \ll B_0$. The Hamiltonian for this system is:

$$H = - \sum_{i=1}^N J_i S_i S_{i+1} - g\mu_B \sigma B \sum_{i=1}^N S_i. \quad (1)$$

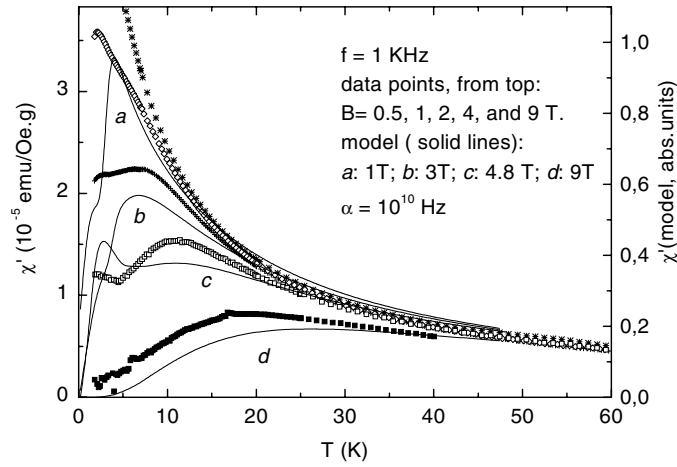


Figure 4. Real part of the ac susceptibility for a range of dc fields and 1 kHz (to convert χ to SI dimensionless units multiply by 57.56). Also shown are the simulated curves for the Ising ring model described in the text.

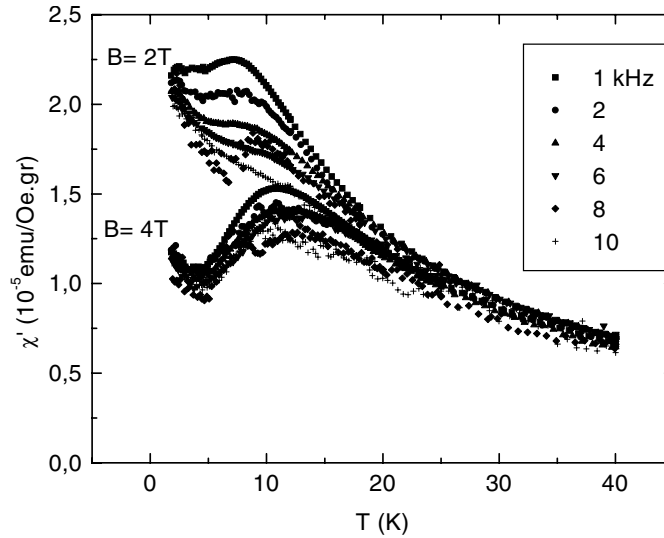


Figure 5. Measurements of ac susceptibility for a range of frequencies for $B = 2$ and 4 T (to convert χ to SI dimensionless units multiply by 57.56).

Here $\sigma = 2$ is the actual total spin of an Fe^{2+} ion, $g = 2$ and μ_B is Bohr's magneton. The values of the fractional spins (S) are $S_i = \pm 1$. The calculation of the ac susceptibility for a random-coupling Ising chain was previously carried out by Reger and Binder [4], using the Glauber master equation [8] in which only single spin-flip steps are taken into account. This master equation is:

$$\frac{d}{dt}P(S_1, \dots, S_N; t) = - \sum_j W_j(S_j \rightarrow -S_j)P(S_1 \dots S_j \dots S_N; t) \\ + \sum_j W_j(-S_j \rightarrow S_j)P(S_1 \dots -S_j \dots S_N; t).$$

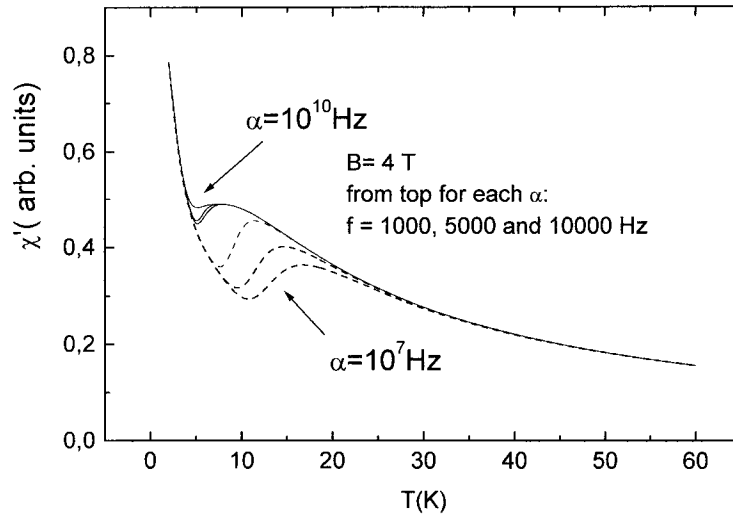


Figure 6. Simulated curves displaying the dependence on frequency of the calculated susceptibility for two values of the attempt frequency α .

Here $P(S_1 \dots S_N; t)$ is the probability of a given configuration of $N = 5$ spins, with a total of $2^5 = 32$ configurations; $W_j(S_j \rightarrow -S_j)$ is the single spin-flip transition probability per unit time for a configuration j , $j = 1, \dots, 32$. In order that detailed balance restrictions are satisfied in the equilibrium state, W_j has the form (here we drop the index j for simplicity) [4, 8]:

$$W(S_i \rightarrow -S_i) = \frac{\alpha}{2} \left\{ 1 - \beta S_i + \frac{1}{2}(\beta - S_i) [(S_{i-1} + S_{i+1}) \tanh(\gamma^+) + (S_{i-1} - S_i) \tanh(\gamma^-)] \right\}. \quad (2)$$

Here $\beta = \tanh(\mu_B g \sigma B_0 / k_B T)$, and for each i the parameters $\gamma^\pm = \tanh((J_{i-1} \pm J_i) / k_B T)$. The P can be written in vector notation, so that the master equation becomes:

$$\frac{d}{dt} |P\rangle = L |P\rangle. \quad (3)$$

Here L is a matrix whose coefficients are [10] $\langle m | L | n \rangle = W(n \rightarrow m) - \delta_{mn} \sum_j W(n \rightarrow j)$, where m and n are the indices of the 32 possible configurations. Of course the restriction of single-flip kinetics considerably reduces the number of nonzero elements of the L matrix. The solution of equation (3) yields $|P(t)\rangle = \exp(Lt) |P(0)\rangle$. One defines a magnetization vector $|M(0)\rangle$, whose components are the magnetic moments M_i of the 32 configurations of spins. If one defines also a complete basis set of 32 unitary and orthonormal vectors $|i\rangle$, the vector $|M(0)\rangle$ can be written as a diagonal matrix $M = \sum_i |i\rangle M_i \langle i|$. The vector $|P(t)\rangle$ can be written as the sum of vectors $P_i(t) |i\rangle$, and thus the thermal average of the magnetization of the ring will be

$$\langle \langle M(t) \rangle \rangle = \langle \langle M P_i(t) \rangle \rangle = \langle \langle M \exp(Lt) P_i(0) \rangle \rangle \quad (4)$$

where $| \rangle = \sum_i |i\rangle$.

The ac susceptibility is defined in terms of the Fourier transform of the time-dependent magnetization correlations,

$$\chi = \frac{1}{k_B T} \int_0^\infty \{ \langle \langle M(t) \dot{M}(0) \rangle \rangle - \langle \langle M(t) \rangle \rangle \langle \langle \dot{M}(0) \rangle \rangle \} \exp(i\omega t) dt \quad (5)$$

where

$$\langle\langle \dot{M}(t) \dot{M}(0) \rangle\rangle = \langle |M P_i(t) L M| \rangle = \langle |M \exp(Lt) L M P_i(0)| \rangle \quad (6a)$$

and

$$\langle\langle \dot{M}(0) \rangle\rangle = \langle |M L P_i(0)| \rangle. \quad (6b)$$

Here we used the results $\dot{M} = [M, L]$ and $\langle |L = 0$ this latter one imposed by the detailed balance condition [4, 10]. Fourier transforming equation (5), taking account of equations (6a) and (6b), gives:

$$\chi = \frac{1}{k_B T} \{ \langle |M(L + i\omega I)^{-1} L M P_i(0)| \rangle - \langle |M(L + i\omega I)^{-1} P_i(0)| \rangle \langle |M L P_i(0)| \rangle \} \quad (7)$$

(where I is the identity matrix). Equation (7) yields the complex susceptibility $\chi = \chi' + i\chi''$ as a function of dc field, frequency and temperature.

5. Discussion

Figure 4 shows a comparison of a set of experimental results with the model calculations, with parameters $\alpha = 10^{10}$ Hz, $J_i/k_B = (-10, 6, -2, 1, -1)$ K, for the same frequency $f = 1$ kHz, and for dc fields in the same range as adopted in the experiments. In spite of the simplicity of the model, the main features are reproduced. For low dc fields the data decrease monotonically with temperature. As the dc field increases beyond 1 T the experimental data display a peak and a shoulder as temperature decreases below 15 K, which eventually evolve into two peaks apparent at $B = 4$ T. The simulations, carried out for a single set of J_i values, display similar features at approximately the same positions as the peaks/shoulders in the data. It seems that the undulations in the actual data are smoothed by averaging over the possible combinations of J_i , whereas the model calculations were restricted to a single set of values. The use of variable coupling constants J_i along the ring is physically justifiable by the number of possible arrangements between neighbouring Fe ions. We have carried out simulations with uniform coupling constants also, and observed that the low temperature structure is not reproduced. Rather, a single, broad peak is observed (similar to the data for 9 T shown in figure 4). We decided to check also whether the undulations might be related to a phase transition of the spin system. We carried out zero field and field cooled dc magnetization measurements for $B = 2$ and 4 T, but no hysteresis was observed, which rules out a phase transition to a glassy state, for instance.

Although the electronic band structure of the H-phase has never been calculated or measured directly, the effects of doping with iron can be understood by comparison with information available for perovskites and the ReO₃ compound [11]. H-Nb₂O₅ has a structure derived from ReO₃ by crystallographic shear. In ReO₃ the valence band has oxygen p character and is located at approximately -14 eV. The d orbital energy for Fe is -16.5 eV [11]. Even considering the differences between these compounds, the Fe electron levels must remain deep underneath the oxygen valence states, and thus form bound states in the structure. This justifies the use of the localized-electron Hamiltonian adopted in the calculations.

It is possible to obtain a qualitative explanation for the variable values obtained for the coupling constants. According to Goodenough [12], the presence of Fe (and possibly also Nb) ions in octahedral sites may result in a range of anion-mediated superexchange interactions. Octahedral Fe ions ($d^6: t_{2g}^4 e_g^2$) may form 180° Fe–O–Fe chains along the channels, besides other possible arrangements like 180° Nb–O–Fe (such Nb⁴⁺ ions ($d^1: t_{2g}^1 e_g^0$) might be displaced from a tetrahedral to an octahedral position), and 90° Fe–Fe coupling for two octahedral sites at

the same level. The sign and strength of such interactions has been estimated by Goodenough [12]: Fe–O–Fe superexchange interactions should be strong and antiferromagnetic, in view of correlation and delocalization exchange effects enhanced by half-filled e_g Fe orbitals each side of the linking oxygen. Nb–O–Fe interactions should be ferromagnetic and weaker in strength, since the Nb ions have empty e_g orbitals. When two Fe occupy octahedral sites at the same level the interaction is ferromagnetic, but can be reversed in sign in the case of simultaneous strong Fe–O–Fe 180° interactions. The strength of Nb–O–Nb coupling should be negligible, since the e_g orbitals are empty and orbital t has a single electron. There might be other possibilities, involving longer distances and different bond angles between cations, but these are much more difficult to estimate. However, the experimental data are consistent with such a wide range of interaction energies between the cations in the channels.

6. Conclusions

We have doped the compound H-Nb₂O₅ with a small amount of Fe, so that some of the empty octahedral sites aligned along the channels of this structure would be filled, forming one-dimensional magnetic arrays. Low temperature ac susceptibility measurements gave results consistent with the formation of linear arrays of spins, with variable coupling constants along the chains. The low temperature undulations in the ac susceptibility were reproduced by a simple Ising ring model of five spins with variable coupling between spins, and by assuming a single spin-flip Glauber kinetics in the calculation of the theoretical susceptibility. Coupling between Fe ions is mediated by the O anions, and the different arrangements available for the cations justify the presence of both ferro- and antiferromagnetic interactions along the chains.

Acknowledgment

This work was partially financed by the Brazilian Ministry of Science and Technology under the contract PRONEX/FINEP/CNPq No 41.96.0907.00.

References

- [1] Paduan A, Becerra C C and Palacio F 1998 *Phys. Rev. B* **58** 3197
Cheikhrouhou A, Dupas C and Renard J P 1983 *J. Physique Lett.* **44** L777
Jacobs I S, Bray J W, Hart H R Jr, Interrante L V, Kasper J S, Watkins G D, Prober D E and Bonner J C 1976 *Phys. Rev. B* **14** 3036
- [2] Pouget J P, Regnault L P, Ain M, Hennion B, Renard J P, Veillet P, Dhahenne G, and Revcolevschi A 1994 *Phys. Rev. Lett.* **72** 4037
- [3] Shiozaki I 1998 *J. Phys.: Condens. Matter* **10** 9813
- [4] Reger J D and Binder K 1985 *Z. Phys. B* **60** 137
- [5] Schäfer H, Gruhn R and Schulte F 1966 *Angew. Chem. (Int. Edn.)* **5** 40
- [6] Anderson J S, Browne J M, Cheetham A K, von Dreele R, Hutchison J L, Lincoln F J, Bevan D J M and Strachle J 1973 *Nature* **243** 81
- [7] Schilling O F 1986 *J. Phys. Chem. Solids* **47** 595
- [8] Glauber R J 1963 *J. Math. Phys.* **4** 294
- [9] Rüscher C H and Nygren M 1991 *J. Phys.: Condens. Matter* **3** 3997
- [10] Kawasaki K 1972 *Phase Transitions and Critical Phenomena* vol 2, ed C Domb and M S Green (London: Academic) p 443
- [11] Harrison W A 1989 *Electronic Structure and the Properties of Solids* (New York: Dover)
- [12] Goodenough J B 1963 *Magnetism and the Chemical Bond* (New York: Wiley)